



This is a repository copy of *Two-stage adaptive robust model for AC network-constrained unit commitment in power systems with uncertain wind power*.

White Rose Research Online URL for this paper:

<https://eprints.whiterose.ac.uk/223671/>

Version: Accepted Version

---

**Article:**

Wang, S., Zhang, X. [orcid.org/0000-0002-6063-959X](https://orcid.org/0000-0002-6063-959X), Du, M. et al. (1 more author) (2025) Two-stage adaptive robust model for AC network-constrained unit commitment in power systems with uncertain wind power. *IEEE Transactions on Sustainable Energy*. pp. 1-13. ISSN 1949-3029

<https://doi.org/10.1109/tste.2025.3542899>

---

© 2025 The Authors. Except as otherwise noted, this author-accepted version of a journal article published in *IEEE Transactions on Sustainable Energy* is made available via the University of Sheffield Research Publications and Copyright Policy under the terms of the Creative Commons Attribution 4.0 International License (CC-BY 4.0), which permits unrestricted use, distribution and reproduction in any medium, provided the original work is properly cited. To view a copy of this licence, visit <http://creativecommons.org/licenses/by/4.0/>

**Reuse**

This article is distributed under the terms of the Creative Commons Attribution (CC BY) licence. This licence allows you to distribute, remix, tweak, and build upon the work, even commercially, as long as you credit the authors for the original work. More information and the full terms of the licence here:

<https://creativecommons.org/licenses/>

**Takedown**

If you consider content in White Rose Research Online to be in breach of UK law, please notify us by emailing [eprints@whiterose.ac.uk](mailto:eprints@whiterose.ac.uk) including the URL of the record and the reason for the withdrawal request.



[eprints@whiterose.ac.uk](mailto:eprints@whiterose.ac.uk)  
<https://eprints.whiterose.ac.uk/>

# Two-stage Adaptive Robust Model for AC Network-Constrained Unit Commitment in Power Systems with Uncertain Wind Power

Siqi Wang, Xin Zhang, *Senior Member, IEEE*, Min Du, *Member, IEEE*, Wei Pei, *Member, IEEE*

**Abstract**— With wind power being extensively integrated into power systems, its inherent uncertainty and variability pose significant challenges to the power system operational security. Traditional robust optimization methods capture the worst-case scenario, which results in overly conservative decisions, with insufficient considerations on AC network constraints in power systems. To overcome this issue, this paper proposes a novel adaptive robust AC network-constrained unit commitment (AC-NCUC) model that considers both the AC network security and the uncertainty of wind power output in power systems. More specifically, a convex polyhedral uncertainty set is constructed to characterize the uncertain wind power output. Here, the conservativeness of UC dispatch decisions can be adjusted by modifying the size of the convex polyhedral uncertainty set. Then, we combine Benders’ decomposition and Newton-Raphson methods to solve the AC-NCUC model for the optimal dispatch decisions. Simulation results on the modified IEEE 6-bus and IEEE RTS 79 systems validate the rationality and validity of our proposed approach. The proposed AC-NCUC model effectively maintains the system security while ensuring economic effectiveness.

**Index Terms**— Adaptive robust optimization, convex polyhedral uncertainty set, AC network-constrained unit commitment, Benders’ decomposition, Newton-Raphson, uncertain wind power.

## NOMENCLATURE

### Constants and Parameters

$b, d, i, l$	Index of buses/loads/units/lines.
$t$	Index of time periods.
$w$	Index of wind farms.
$dP_0, dQ_0$	Initial active/reactive power mismatch vector.
$DR_i, UR_i$	Ramp-down/ -up rate limit for unit $i$ .

This work was supported in part by the Royal Society International Exchanges under Grant IEC\NSFC\242449, in part by the U.K. Research and Innovation Future Leaders Fellowship “Digitalisation of Electrical Power and Energy Systems Operation” under Grant MR/W011360/2, and in part by the U.K. Engineering and Physical Sciences Research Council New Investigator Award under Grant EP/W028905/1. (*Corresponding author: Xin Zhang, Min Du.*)

S. Wang is with the Institute of Electrical Engineering, Chinese Academy of Sciences, and with the School of Electrical and Electronic Engineering, University of Sheffield, Sheffield, S10 2TN, United Kingdom. (e-mail: wangsiqi@mail.iee.ac.cn).

X. Zhang and M. Du are with the School of Electrical and Electronic Engineering, University of Sheffield, Sheffield, S10 2TN, United Kingdom. (e-mail: m.du@sheffield.ac.uk; xin.zhang1@sheffield.ac.uk).

W. Pei is with the Institute of Electrical Engineering, Chinese Academy of Sciences, Beijing 100190, China. (peiwei@mail.iee.ac.cn).

NB, ND, NG	Number of buses/ loads/ units.
NL, NT, NW	Number of lines/ time periods/ wind farms.
<b>KD, KL, KP, KW</b>	Bus-load/ -line/ -unit/ -wind farm incidence matrix.
$P^d$	System demand vector.
$P^w$	Forecasted wind power output vector.
$P_{dt}$	System demand of load $d$ at time $t$ .
$\underline{P}_i, \bar{P}_i$	Minimum/Maximum active power output of unit $i$ .
$\bar{P}_{wt}$	Forecasted power output of wind farm $w$ at time $t$ .
$\hat{P}_{wt}$	Forecasted power output variation of wind farm $w$ at time $t$ .
$\underline{Q}_i, \bar{Q}_i$	Minimum/Maximum reactive power output of unit $i$ .
<b>SF</b>	Shift factor.
$SU_{it}, SD_{it}$	Startup/Shutdown cost of unit $i$ at time $t$ .
$U_{it}$	Commitment cost of unit $i$ at time $t$ .
$T_i^{on}, T_i^{off}$	Minimum up/down time of unit $i$ .
$\lambda$	Wind power output fluctuation parameter.
$\Delta$	Uncertainty budget.
$\Lambda$	Decimal part of uncertainty budget parameter $\Delta$ .
$[\Delta^t]$	Integer part of uncertainty budget parameter $\Delta$ at time $t$ .
$T_{max}, T_{min}$	Maximum/Minimum vector of transformer taps.
$V_{max}, V_{min}$	Maximum/Minimum vector of voltage magnitude.
$\Delta Q_{max}, \Delta Q_{min}$	Maximum/Minimum vector of unit reactive power output increment.
$X_{i(t-1)}^{on}, X_{i(t-1)}^{off}$	ON/OFF time of unit $i$ at time $t$ .
$\mathcal{W}$	Uncertainty set of wind power output.
$\mathcal{Y}_{max}, \mathcal{Y}_{min}$	Lower/Upper limit vector of phase shifter angle.
$F_{max}$	Maximum vector of active power flow.
$F_0$	Initial active power flow vector.
$T_0$	Initial transformer tap vector.
$V_0$	Initial bus voltage vector.
$\gamma_0$	Initial phase shifter angle vector.
<b>H, L, E, G, M, N, R, S</b>	Jacobian matrix.
<b>U, W, Y, Z</b>	Jacobian submatrices.
<b>Variables</b>	
$F, \Delta F$	Active power flow vector and its increment.
$T, \Delta T$	Transformer tap vector and its increment.

$V, \Delta V$	Bus voltage vector and its increment.
$I$	Unit state vector.
$I_{it}$	Binary variable to indicate if unit $i$ is on at time $t$ .
$y_{it}$	Binary variable to indicate if unit $i$ is start-up at time $t$ .
$z_{it}$	Binary variable to indicate if the unit $i$ is shutdown at time $t$ .
$L_{d,t}^{SH}$	Load shedding of load $d$ at time $t$ .
$MP_{b1}, MP_{b2}$	Positive slack variables of active power mismatch at bus $b$ .
$MQ_{b1}, MQ_{b2}$	Positive slack variables of reactive power mismatch at bus $b$ .
$P^g$	Active power output vector of unit.
$P_{it}$	Active power output of unit $i$ at time $t$ .
$P_{wt}$	Active power output of wind farm $w$ at time $t$ .
$\gamma, \Delta \gamma$	Phase shifter angle vector and its increment.
$\Delta P, \Delta Q$	Active/Reactive power increment vector.
$\Delta \theta$	Bus phase angle increment vector.
$\tau, \gamma, \eta$	Dual variables.
$\pi, \underline{\psi}, \bar{\psi}$	Simplex multiplier vector.
$\bar{\varphi}_{wt}, \underline{\varphi}_{wt}, \bar{\lambda}_{wt}, \underline{\lambda}_{wt}$	Auxiliary continuous variables.
$\bar{\alpha}_{wt}, \underline{\alpha}_{wt}, \bar{\mu}_{wt}, \underline{\mu}_{wt}$	Auxiliary binary variables.

## I. INTRODUCTION

WIND power offers sustainability and zero-carbon emissions, making it a competitive alternative to traditional energy sources. According to the International Renewable Energy Agency report, the cumulative capacity of installed wind power worldwide reached 1,017 gigawatts (GW) by the end of 2023 [1], representing a roughly 135-fold increase over the last three decades, up from 7.5 GW in 1997 [2]. Wind power's share of worldwide electricity usage in 2023 reached 7.8%, more than doubling its 3.5% share in 2015 [3]. The rapid growth of wind power fosters sustainable energy development, but also poses considerable challenges to power system stability, security, and cost-effectiveness due to the inherent intermittency and uncertainty of wind power output [4-6].

The core element for achieving a secure and cost-effective power system operation is the unit commitment (UC) dispatch decision. It provides a physically optimal solution to minimize the operation cost while ensuring the security and stability of power system operation [7]. However, the performance of UC dispatch decisions can be compromised when actual wind power output deviates from its forecasted values. To address this, a network-constrained unit commitment (NCUC) model considering uncertain wind power was proposed to determine resilient decisions. Stochastic programming (SP) [8-12] and robust optimization (RO) [13-18] are representative approaches that have been widely utilized to NCUC under various uncertain conditions. The SP method typically utilizes prior probability distribution functions (PDFs) to generate numerous scenarios presenting wind power uncertainty. It requested on substantial historical data, and the computational complexity of handling large scenario sets often renders SP intractable [19]. Although scenario selection techniques were used to reduce the huge

computational burden, these methods were at risk of ignoring certain critical scenarios, which potentially resulted in a compromised power system performance against uncertainties [20, 21]. In contrast, RO eliminated the need for prior knowledge of PDFs, which made the RO method advantageous when historical information was limited [22]. However, it might yield excessively conservative UC dispatch decisions as it only considered the worst-case scenario with a low-probability occurrence [23]. To overcome these aforementioned issues, the adaptive robust optimization (ARO) method [24] was proposed. The ARO approach can effectively characterize the uncertain variables with limited information while allowing for the adjustment of the conservativeness of the UC dispatch decisions. Consequently, the ARO method was widely integrated into UC models to deal with uncertain wind power output. For example, the authors in [25, 26] utilized the ARO method to tackle the uncertainty of wind power output in the UC model to determine more appropriate dispatch decisions.

However, the UC problem with uncertain variables usually incorporates DC network constraints (DC-UC) rather than AC network constraints (AC-UC) [27]. DC-UC models do not account for voltage magnitude and reactive power constraints, which cannot fully capture the physical properties of the network, leading to voltage instability and major blackouts [28]. As a result, the dispatch decisions derived from DC-UC models cannot ensure the AC network-related power system security. In practice, most real-world power systems are AC systems, where the AC network constraints (such as voltage and reactive power) are generally considered to determine more practical dispatch decisions. This indicates that it is especially critical to maintain voltage security and provide reactive power support for power systems. To address this issue, an AC-UC model was developed in [29] to incorporate voltage and reactive power constraints in order to deliver more practical dispatch decisions while ensuring power system security. However, this AC-UC model did not consider uncertain wind power output. With the growing penetration of wind power in modern power systems, the application of this AC-UC model is limited because its dispatch decisions may be insufficient to perform effectively in power systems due to the variability of wind power. In this context, a network-constrained AC-UC model was proposed in [30], which considered the uncertainty of wind power based on the stochastic robust approach. However, this model relies on numerous wind power scenarios, which results in a significant computational burden. In addition, solving this model in [30] remains challenging due to its mixed-integer nonlinear and non-convex nature. Then, the authors in [31] introduced an ARO-based AC-UC model to determine the UC dispatch decisions for power systems with uncertain wind power output, where an uncertainty set was designed to depict the wind power output uncertainty. Thus, this model eliminates the need to generate a large number of wind power output scenarios. However, the budget parameter in the uncertainty set, which is integer-constrained, limits its ability to represent wind power output accurately. Moreover, the model's nonlinear characteristics make it difficult to solve analytically. In addition, this ARO-based AC-UC model is insufficient to completely capture the interactions among active and reactive power, power flows, phase shifts, bus voltages, and tap-changing transformers.

To overcome the shortcomings of existing approaches, this

paper presents a novel adaptive robust AC network constrained unit commitment (AC-NCUC) model to determine the most optimal UC dispatch decisions for power systems under wind power uncertainty. The AC-NCUC model can accurately reflect the physical properties of power systems. Especially for uncertain wind power output, a convex polyhedral uncertainty set is designed, allowing the uncertainty budget parameter to take decimal values, thereby better capturing the wind power output uncertainty. To solve the overall problem, the proposed AC-NCUC model is decomposed into an outer master problem with DC-UC and an AC subproblem. Then, Benders' decomposition and Newton-Raphson methods are employed iteratively to solve them for the optimal solution. The key contributions are outlined as follows:

- 1) This paper constructs a convex polyhedral uncertainty set to characterize uncertain wind power. The size of this uncertainty set can be adjusted to control the conservativeness of the dispatch scheme, providing a flexible and practical dispatch strategy for system operators. In addition, the budget parameter of the uncertainty set is extended to allow decimal values.
- 2) This paper proposes a two-stage "min-max-min" model for the AC-UC problem to obtain a practical UC dispatch strategy under extreme wind power output scenarios within the convex polyhedral uncertainty set. To solve this model, this overall AC-UC problem is decomposed into an outer master problem and an AC subproblem, allowing for an effective solution.
- 3) To determine the globally optimal dispatch decision, we integrate Benders' decomposition with the full Newton-Raphson method to search for the UC decisions. Extensive case studies on two modified IEEE systems validate the proposed approach, demonstrating its effectiveness in balancing system security and economic costs.

The remaining part of this paper is structured as follows: Section II introduces the framework of the proposed AC-NCUC model and elaborates on its mathematical formulation. Section III introduces the solution algorithm, Section IV implements case studies, and Section V draws conclusions.

## II. ADAPTIVE ROBUST AC NETWORK CONSTRAINED UNIT COMMITMENT MODEL

### A. Overall Framework

The proposed AC-NCUC model is a two-stage unit commitment problem, which aims to determine optimal dispatch decisions to minimize the total cost [32]. More specifically, the total cost is the sum of the here-and-now decision costs and the wait-and-see decision costs. In the first stage, here-and-now decisions, including on/off status, startup and shutdown of units are determined to ensure the secure power system operation. In the second stage, after the here-and-now decisions are determined, power output of units, load shedding, as well as wind power curtailment are optimized considering extreme wind power output scenarios and AC network constraints, where these decisions in the second stage are defined as wait-and-see decisions. Thus, the overall framework of the proposed model is depicted in Fig. 1.

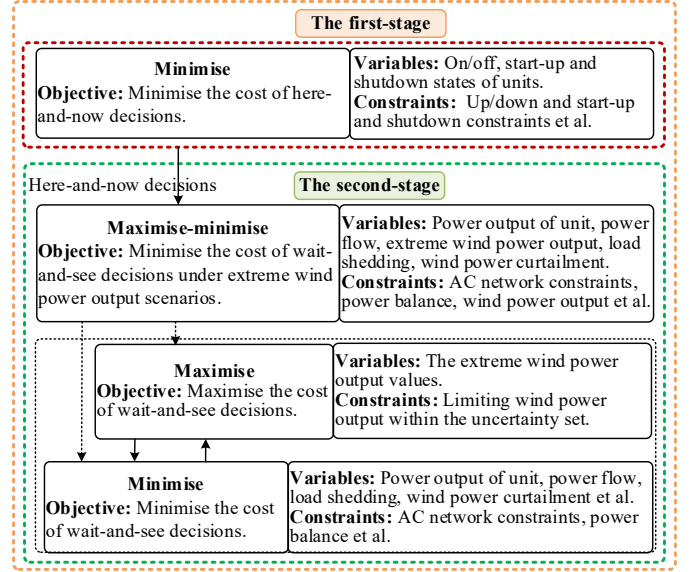


Fig. 1. Overall framework of the proposed AC-NCUC model.

### B. Convex Polyhedral Uncertainty Set

Traditional adaptive robust methods in [33, 34] characterize uncertain wind power output through an uncertainty set with an integer-valued uncertainty budget parameter. This approach restricts the representation of wind power output due to the inherent limitation of integer-only uncertainty budget parameters. To overcome this issue, we construct a convex polyhedral uncertainty set that allows the uncertainty budget parameter to take decimal values. This convex polyhedral uncertainty set can capture more precise representation of wind power variability and is formulated as follows:

$$\mathcal{W} = \left\{ \begin{array}{l} P_{wt} \in \mathbb{R}^{NW}, \forall w, \forall t \\ \sum_{w=1}^{NW} \left| \frac{P_{wt} - \bar{P}_{wt}}{\hat{P}_{wt}} \right| \leq \Delta^t \\ P_{wt} \in [\bar{P}_{wt} - \hat{P}_{wt}, \bar{P}_{wt} + \hat{P}_{wt}] \\ \Lambda = \Delta^t - \lfloor \Delta^t \rfloor \\ 0 \leq \Delta^t \leq NW, 0 \leq \Lambda \leq 1 \end{array} \right\} \quad (1)$$

where  $P_{wt}$  represents the actual wind power output, which lies within the range of  $[\bar{P}_{wt} - \hat{P}_{wt}, \bar{P}_{wt} + \hat{P}_{wt}]$ .  $\Delta^t$  represents a uncertainty budget parameter of the uncertainty set at time  $t$ , which can effectively control the size of the convex polyhedral uncertainty, thereby adjusting the conservativeness of the proposed AC-NCUC model.  $\lfloor \Delta^t \rfloor$  is the integer and rounded down value of  $\Delta^t$ .  $\Lambda$  denotes the decimal difference between  $\Delta^t$  and  $\lfloor \Delta^t \rfloor$ , which is a decimal auxiliary parameter. As such,  $\mathcal{W}$  is formulated as a convex polyhedral uncertainty set, capturing all possible wind power output scenarios at time  $t$ . The introduced decimal auxiliary parameter  $\Lambda$  can effectively improve the precision and adaptability of the wind power output uncertainty set.

### C. Mathematical Formulation

Thus, the mathematical formulation of the proposed AC-NCUC model is presented as follows:

$$\min_{I_{it}, y_{it}, z_{it}} \sum_{t=1}^{NT} \sum_{i=1}^{NG} (U_{it} I_{it} + S U_{it} y_{it} + S D_{it} z_{it}) + \max_{P_{wt} \in \mathcal{W}} \min_{P_{wt} \in \mathcal{W}} \left[ \sum_{t=1}^{NT} \left[ \sum_{i=1}^{NG} F_{ci}(P_{it}) + \sum_{b=1}^{ND} C^L L_{bt}^{SH} + \sum_{w=1}^{NW} C^W P_{wt}^{SP} \right] \right] \quad (2)$$

$$y_{it} - z_{it} = I_{it} - I_{i(t-1)} \quad \forall i, \forall t \quad (3)$$

$$y_{it} + z_{it} \leq 1 \quad \forall i, \forall t \quad (4)$$

$$\left[ X_{i(t-1)}^{on} - T_i^{on} \right] \cdot [I_{i(t-1)} - I_{it}] \geq 0 \quad \forall i, \forall t \quad (5)$$

$$\left[ X_{i(t-1)}^{off} - T_i^{off} \right] \cdot [I_{it} - I_{i(t-1)}] \geq 0 \quad \forall i, \forall t \quad (6)$$

$$\sum_{i=1}^{NG} P_{it} + \sum_{w=1}^{NW} (P_{wt} - P_{wt}^{SP}) + \sum_{d=1}^{ND} L_{dt}^{SH} = \sum_{d=1}^{ND} P_{dt} \quad \forall t \quad (7)$$

$$\underline{P}_i I_{it} \leq P_{it} \leq \bar{P}_i I_{it} \quad \forall i, \forall t \quad (8)$$

$$\underline{Q}_i I_{it} \leq Q_{it} \leq \bar{Q}_i I_{it} \quad \forall i, \forall t \quad (9)$$

$$P_{it} - P_{i(t-1)} \leq UR_i (1 - y_{it}) + \underline{P}_i y_{it} \quad \forall i, \forall t \quad (10)$$

$$P_{i(t-1)} - P_{it} \leq DR_i (1 - z_{it}) + \underline{P}_i z_{it} \quad \forall i, \forall t \quad (11)$$

$$\mathbf{SF} \cdot (\mathbf{KW} \cdot (\mathbf{P}^W - \Delta \mathbf{P}^W) + \mathbf{KP} \cdot \mathbf{P}^g - \mathbf{KD} \cdot \mathbf{P}^d) = \mathbf{F} \quad (12)$$

$$|\mathbf{F}| \leq \mathbf{F}_{\max} \quad (13)$$

$$\mathbf{V}_{\min} \leq \mathbf{V} \leq \mathbf{V}_{\max} \quad (14)$$

$$\mathbf{T}_{\min} \leq \mathbf{T} \leq \mathbf{T}_{\max} \quad (15)$$

$$\mathbf{Y}_{\min} \leq \mathbf{Y} \leq \mathbf{Y}_{\max} \quad (16)$$

where the objective function (2) minimizes the total cost, including unit commitment, power output, wind power curtailment and load shedding costs, under extreme wind power output scenarios over the entire time period NT. Constraints (3)-(4) indicate the start-up and shutdown limitations of all units. Constraints (5)-(6) indicate the minimum up-time and down-time limitations for all units. Constraint (7) ensures power balance throughout the system. Constraints (8)-(9) represent the active and reactive power output capacity limitations for all units. Constraints (10)-(11) define ramping up and ramping down limits. Constraint (12) describes the power flow on lines, and constraint (13) limits the power flow capacity. Constraints (14)-(16) limit the voltage, tap-changing transformer and phase-shifting transformer capacities, respectively. Note that the ON/OFF cost of unit  $i$  is set to 0.

#### D. Compact Formulation

To facilitate the developed solution algorithm in the next section, we reformulate the AC-NCUC model (2)-(16) to a compact form as follows:

$$\min_{\mathbf{x} \in \mathcal{X}} \mathbf{c}^T \mathbf{x} + \max_{\mathbf{w} \in \mathcal{W}} \min_{\mathbf{y} \in \Omega(\mathbf{x}, \mathbf{w})} \mathbf{b}^T \mathbf{y} \quad (17)$$

$$\text{s.t. } \mathbf{Y} \mathbf{x} \leq \mathbf{f} \quad \forall \mathbf{x} \in \mathcal{X} \quad (18)$$

$$\mathbf{H} \mathbf{y}(\mathbf{w}) \leq \mathbf{h} \quad \boldsymbol{\tau} \quad \forall \mathbf{w} \in \mathcal{W} \quad (19)$$

$$\mathbf{A} \mathbf{x} + \mathbf{B} \mathbf{y}(\mathbf{w}) \leq \mathbf{g} \quad \boldsymbol{\varphi} \quad \forall \mathbf{w} \in \mathcal{W} \quad (20)$$

$$\mathbf{I}_u \mathbf{y}(\mathbf{w}) - \mathbf{w} = \mathbf{m} \quad \boldsymbol{\eta} \quad \forall \mathbf{w} \in \mathcal{W} \quad (21)$$

where vector  $\mathbf{x}$  denotes the UC dispatch decision variables in the first stage, and vector  $\mathbf{y}(\mathbf{w})$  indicates the dispatch decisions in the second stage. The matrix  $\mathbf{Y}$  and vector  $\mathbf{f}$  refer to the coefficient matrices and constant vectors in constraints (3)-(6),

respectively. Similarly, matrices  $\mathbf{H}, \mathbf{A}, \mathbf{B}, \mathbf{I}_u$  and vectors  $\mathbf{h}, \mathbf{g}, \mathbf{m}$  are equivalent to the coefficient matrices and constant vectors in constraints (7)-(16), respectively. Note that  $\mathbf{w}$  is the wind power output vector, which belongs to the convex polyhedral uncertainty set  $\mathcal{W}$ . Additionally,  $\boldsymbol{\tau}, \boldsymbol{\varphi}$  and  $\boldsymbol{\eta}$  are dual variable vectors of constraints (19)-(21).

### III. SOLUTION METHODOLOGY

This section combines Benders' decomposition and Newton-Raphson methods to solve the proposed AC-NCUC model. Firstly, the Benders' decomposition algorithm is applied to decompose the proposed AC-NCUC model into an outer master problem and an AC subproblem. Then, the AC subproblem is iteratively solved by the Newton-Raphson method. The proposed solution algorithm is detailed as follows:

#### A. Outer Master Problem

The outer master problem is a two-stage UC model with DC network constraints. This problem determines dispatch strategies, which are then used to check the AC network security subproblem. Here, the outer master problem is required to be decomposed into an inner master problem and a DC network security subproblem through the Benders' decomposition algorithm. Based on the initial feasible values, the formulation of the inner master problem is as follows:

$$\min_{\mathbf{x} \in \mathcal{X}} \mathbf{c}^T \mathbf{x} + \boldsymbol{\alpha} \quad (22)$$

$$\text{s.t. } \mathbf{Y} \mathbf{x} \leq \mathbf{f} \quad \forall \mathbf{x} \in \mathcal{X} \quad (23)$$

$$\boldsymbol{\alpha} \geq \max_{\mathbf{w} \in \mathcal{W}} \min_{\mathbf{y} \in \Omega(\mathbf{x}, \mathbf{w})} \mathbf{b}^T \mathbf{y} \quad (24)$$

where constraint (24) represents a Benders cut condition, which is usually categorized into two types according to the DC network security subproblem: 1) optimal cut, and 2) feasible cut.

1) **An optimal cut:** If the DC network security subproblem is feasible at a certain iteration, an optimal cut is added to the inner master problem as an additional constraint, as described below:

$$\boldsymbol{\alpha} \geq \max_{\boldsymbol{\varphi}, \boldsymbol{\tau}, \boldsymbol{\eta}} \boldsymbol{\varphi}^T (\mathbf{A} \mathbf{x} - \mathbf{g}) - \boldsymbol{\tau}^T \mathbf{h} + \boldsymbol{\eta}^T (\mathbf{w} + \mathbf{m}) \quad (25)$$

2) **A feasible cut:** If the DC network security subproblem is infeasible at a certain iteration, a feasibility cut is proposed to be built in the previous iteration [35]. The feasibility cut adjusts the previous solution to ensure that the DC network security subproblem becomes feasible. To generate a feasibility cut, the coupling constraints of the DC network security subproblem (20) are slackened. The slackened problem is measured as either feasible or infeasible for the DC network security subproblem according to the duality theorem. The formulation is described as below:

$$\begin{aligned} \min \mathbf{1}^T \mathbf{s} = E & & \max \boldsymbol{\lambda}^T (\mathbf{g} - \mathbf{A} \hat{\mathbf{x}}) \\ \mathbf{B} \mathbf{y} - \mathbf{s} \leq \mathbf{g} - \mathbf{A} \hat{\mathbf{x}} : \boldsymbol{\lambda} & \Rightarrow & \mathbf{B}^T \boldsymbol{\lambda} \leq \mathbf{0} \\ \mathbf{s} \geq \mathbf{0}; \mathbf{y} \geq \mathbf{0} & & -E \boldsymbol{\lambda} \leq \mathbf{1} \\ & & \boldsymbol{\lambda} \leq \mathbf{0} \end{aligned} \quad (26)$$

When the solution vector of the inner master problem is transferred to the DC network security subproblem, the original subproblem becomes feasible. It can be equivalently considered that the corresponding slackened problem satisfies  $E^* = 0$  (or  $E^* \leq 0, \mathbf{1}^T \mathbf{s}^* = E^*$ ), then the condition for the subproblem in the previous stage is expressed as:

$$\lambda^{T*}(\mathbf{g} - \mathbf{A}\mathbf{x}) \leq 0 \quad (27)$$

where the feasible cut (27) is incorporated into the inner master problem at the previous stage to generate a feasible solution  $\hat{\mathbf{x}}$  for the subproblem.

In addition, the DC network security subproblem is derived using the duality theory, transforming the max-min problem into the following equivalent maximization problem:

$$\mathbf{S}(\mathbf{x}, \mathbf{w}) = \max_{\varphi, \tau, \eta} \varphi^T(\mathbf{A}\mathbf{x} - \mathbf{g}) - \tau^T \mathbf{h} + \eta^T(\mathbf{w} + \mathbf{m}) \quad (28)$$

$$-\varphi^T \mathbf{B} - \tau^T \mathbf{H} + \eta^T \mathbf{I}_u = \mathbf{b} \quad (29)$$

$$\tau \geq \mathbf{0}, \varphi \geq \mathbf{0}, \eta: \text{free} \quad (30)$$

Here,  $\mathbf{S}(\mathbf{x}, \mathbf{w})$  denotes the cost function after the dual transformation, where this function maximizes the dispatch cost subject to DC network constraints. Constraints (29)-(30) exclude the reactive power constraints (i.e., constraints (9)), bus voltage violation (i.e., constraints (14)), tap-changing transformer and phase-shifting transformer constraints (i.e., constraints (15-16)). The nonlinear part  $\eta^T \mathbf{w}$  in (28) can be linearized, which is detailed in the next subsection. As a result, the DC network security subproblem (28)-(30) can be formulated as a mixed-integer linear programming (MILP) problem.

### B. Inner Bilinear Decomposition

After the dual transformation, the objective function (28) contains a nonlinear part as shown by (31):

$$\eta^T \mathbf{w} = \sum_{t=1}^{\text{NT}} \sum_{w=1}^{\text{NW}} P_{wt} \eta_{wt} \quad (31)$$

The DC network security subproblem is to find extreme wind power output scenarios, i.e., the extreme points within the designed convex polyhedral uncertainty set  $\mathcal{W}$ . According to [36], the extreme wind power output  $P_{wt}$  is specifically described as follows:

$$P_{wt} = \bar{P}_{wt} + \hat{P}_{wt}(\bar{\alpha}_{wt} - \underline{\alpha}_{wt}) + \Lambda \hat{P}_{wt}(\bar{\mu}_{wt} - \underline{\mu}_{wt}) \quad (32)$$

$$\sum_{w=1}^{\text{NW}} (\bar{\alpha}_{wt} + \underline{\alpha}_{wt}) = |\Delta| \quad (33)$$

$$\sum_{w=1}^{\text{NW}} (\bar{\mu}_{wt} + \underline{\mu}_{wt}) = 1 \quad (34)$$

$$\Lambda = \Delta^t - |\Delta^t| \quad (35)$$

$$\sum_{w=1}^{\text{NW}} (\bar{\alpha}_{wt} + \underline{\alpha}_{wt}) = |\Delta| \quad (36)$$

$$\sum_{w=1}^{\text{NW}} (\bar{\mu}_{wt} + \underline{\mu}_{wt}) = 1 \quad (37)$$

$$\bar{\alpha}_{wt} + \underline{\alpha}_{wt} + \bar{\mu}_{wt} + \underline{\mu}_{wt} \leq 1 \quad (38)$$

$$\bar{\alpha}_{wt}, \underline{\alpha}_{wt}, \bar{\mu}_{wt}, \underline{\mu}_{wt} \in \{0, 1\} \quad (39)$$

$$\forall w, \forall t \quad (40)$$

Therefore, the nonlinear part (31) can be transformed into a linear term that includes bilinear parts  $\bar{\alpha}_{wt}\eta_{wt}$ ,  $\underline{\alpha}_{wt}\eta_{wt}$ ,  $\bar{\mu}_{wt}\eta_{wt}$  and  $\underline{\mu}_{wt}\eta_{wt}$ . Here, the bilinear part is expressed by a binary variable and a continuous variable, which can be linearized by the big-M method. By introducing auxiliary continuous variables  $\bar{\varphi}_{wt}$ ,  $\underline{\varphi}_{wt}$ ,  $\bar{\lambda}_{wt}$  and  $\underline{\lambda}_{wt}$ , we can obtain:

$$-M\bar{\alpha}_{wt} \leq \bar{\varphi}_{wt} \leq M\underline{\alpha}_{wt} \quad (41)$$

$$-M(1 - \bar{\alpha}_{wt}) \leq \eta_{wt} - \bar{\varphi}_{wt} \leq M(1 - \bar{\alpha}_{wt}) \quad (42)$$

$$-M\underline{\alpha}_{wt} \leq \underline{\varphi}_{wt} \leq M\underline{\alpha}_{wt} \quad (43)$$

$$-M(1 - \underline{\alpha}_{wt}) \leq \eta_{wt} - \underline{\varphi}_{wt} \leq M(1 - \underline{\alpha}_{wt}) \quad (44)$$

$$-M\bar{\mu}_{wt} \leq \bar{\lambda}_{wt} \leq M\bar{\mu}_{wt} \quad (45)$$

$$-M(1 - \bar{\mu}_{wt}) \leq \eta_{wt} - \bar{\lambda}_{wt} \leq M(1 - \bar{\mu}_{wt}) \quad (46)$$

$$-M\underline{\mu}_{wt} \leq \underline{\lambda}_{wt} \leq M\underline{\mu}_{wt} \quad (47)$$

$$-M(1 - \underline{\mu}_{wt}) \leq \eta_{wt} - \underline{\lambda}_{wt} \leq M(1 - \underline{\mu}_{wt}) \quad (48)$$

$$\forall w, \forall t \quad (49)$$

where  $M$  represents the large positive constant. Constraints (41)-(42) are the linearization of  $\bar{\alpha}_{wt}\eta_{wt}$ . Constraints (43)-(49) are the linearized formulations of  $\underline{\alpha}_{wt}\eta_{wt}$ ,  $\bar{\mu}_{wt}\eta_{wt}$  and  $\underline{\mu}_{wt}\eta_{wt}$ , respectively. Finally,  $\eta^T \mathbf{w}$  is reformulated as follows:

$$\sum_{t=1}^{\text{NT}} \sum_{w=1}^{\text{NW}} \left[ \bar{P}_{wt}\eta_{wt} + \hat{P}_{wt}(\bar{\varphi}_{wt} - \underline{\varphi}_{wt}) + (\Delta - |\Delta|)\hat{P}_{wt}(\bar{\lambda}_{wt} - \underline{\lambda}_{wt}) \right] \quad (50)$$

### C. AC Network Security Subproblem

Once the outer master problem has been addressed using the Benders' decomposition algorithm, the obtained initial UC dispatch strategy is transferred to the AC network security subproblem. The AC subproblem is employed to check AC network constraints. These constraints can stabilize the voltage within a specific range to avoid the voltage drop in the remote bus through long lines. Based on the Newton-Raphson method in [29], the AC network security subproblem is solved as follows:

$$\text{Min } L(\hat{\mathbf{i}}, \hat{\mathbf{P}}_g) = \sum_{b=1}^{\text{NB}} (\text{MP}_{b1} + \text{MP}_{b2}) + \sum_{b=1}^{\text{NB}} (\text{MQ}_{b1} + \text{MQ}_{b2}) \quad (51)$$

$$\begin{bmatrix} \text{KP} & \mathbf{0} \\ \mathbf{0} & \text{KP} \end{bmatrix} \begin{bmatrix} \Delta P \\ \Delta Q \end{bmatrix} - \begin{bmatrix} \mathbf{H} & \mathbf{L} & \mathbf{E} & \mathbf{G} \\ \mathbf{M} & \mathbf{N} & \mathbf{R} & \mathbf{S} \end{bmatrix} \cdot \begin{bmatrix} \Delta \theta \\ \Delta V \\ \Delta T \\ \Delta \gamma \end{bmatrix} + \quad (52)$$

$$\begin{bmatrix} \text{MP1} \\ \text{MQ1} \end{bmatrix} - \begin{bmatrix} \text{MP2} \\ \text{MQ2} \end{bmatrix} = \begin{bmatrix} -dP_0 \\ -dQ_0 \end{bmatrix}$$

$$\Delta F = [\mathbf{U} \quad \mathbf{W} \quad \mathbf{Y} \quad \mathbf{Z}] \begin{bmatrix} \Delta \theta \\ \Delta V \\ \Delta T \\ \Delta \gamma \end{bmatrix} \quad (53)$$

$$\Delta P = \mathbf{0} \quad \boldsymbol{\pi} \quad (54)$$

$$\Delta Q_{\min} \leq \Delta Q \leq \Delta Q_{\max} \quad \underline{\boldsymbol{\psi}}, \bar{\boldsymbol{\psi}} \quad (55)$$

$$\mathbf{T}_{\min} - \mathbf{T}_0 \leq \Delta \mathbf{T} \leq \mathbf{T}_{\max} - \mathbf{T}_0 \quad (56)$$

$$\boldsymbol{\gamma}_{\min} - \boldsymbol{\gamma}_0 \leq \Delta \boldsymbol{\gamma} \leq \boldsymbol{\gamma}_{\max} - \boldsymbol{\gamma}_0 \quad (57)$$

$$\mathbf{V}_{\min} - \mathbf{V}_0 \leq \Delta \mathbf{V} \leq \mathbf{V}_{\max} - \mathbf{V}_0 \quad (58)$$

$$-\mathbf{F}_{\max} - \mathbf{F}_0 \leq \Delta \mathbf{F} \leq \mathbf{F}_{\max} - \mathbf{F}_0 \quad (59)$$

where the objective function (51) aims to minimize mismatches in active and reactive power at the buses through the Newton-Raphson method. The slack matrix  $\mathbf{MP}$  and  $\mathbf{MQ}$  refer to active power and reactive power mismatches, with these slack values acting as virtual units introduced to eliminate mismatches. Constraint (52) represents the linearized active and reactive power balance equation. Here,  $dP_0$  and  $dQ_0$  denote mismatches of active and reactive power at the buses. Constraints (53)

represents the linearized active power flow equation. Constraints (54)-(59) define boundaries for active and reactive power output, phase shifter angle, transformer tap position, bus voltage and active power flow, respectively. In addition, the Jacobian matrix formulation with transformer model is presented in the Appendix.

When the objective function  $L(\hat{\mathbf{I}}, \hat{\mathbf{P}}_g)$  exceeds the predefined threshold  $k$ , the outer master problem incorporates the formed Benders cut (60) to mitigate power flow and voltage violations in the subsequent iteration.

$$L(\hat{\mathbf{I}}, \hat{\mathbf{P}}) = \hat{L} + \sum_{i=1}^{NG} \pi_{it}^n (P_{it} I_{it} - \hat{P}_{it} \hat{I}_{it}) + \sum_{i=1}^{NG} \bar{\psi}_{it}^n Q_{i,\max} (I_{it} - \hat{I}_{it}) - \sum_{i=1}^{NG} \psi_{it}^n Q_{i,\min} (I_{it} - \hat{I}_{it}) \leq 0 \quad (60)$$

For simplicity and clarity, the detailed process of the solution algorithm is shown in Fig. 2.

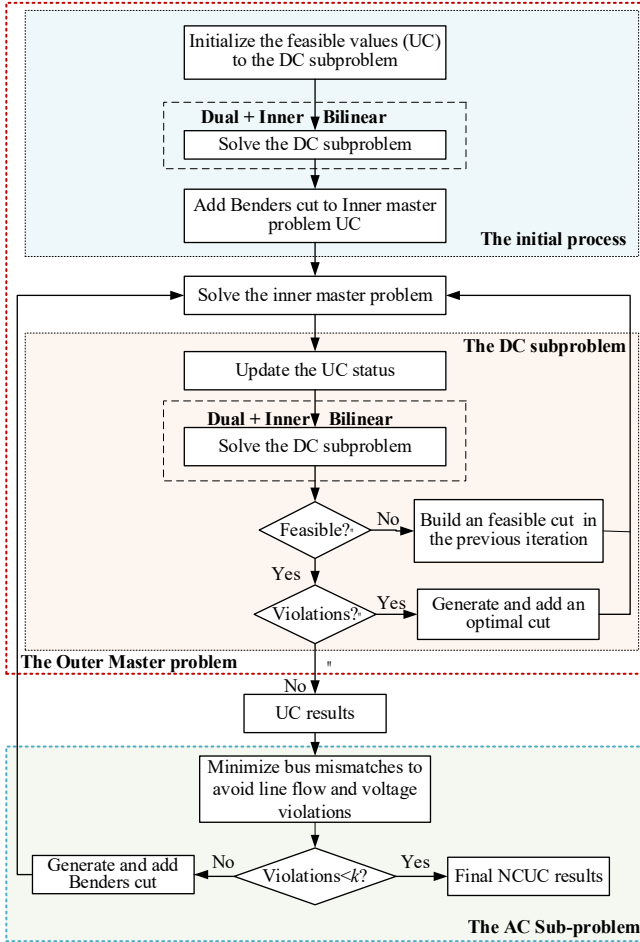


Fig. 2. Overall framework of the proposed solution algorithm.

#### IV. COMPUTATIONAL EXPERIMENTS

To verify the effectiveness of the proposed adaptive robust AC-NCUC model and the associated solution approach, case studies are conducted on the modified IEEE 6-bus system and RTS-79 system. All simulations are performed in MATLAB 2014b using CPLEX 12.5 solver on a laptop equipped with a 2.9GHz CPU and 8 GB of RAM. The predefined threshold  $k = 0.001$  to meet the final NCUC results criteria.

#### A. IEEE 6-bus System

The modified IEEE 6-bus system consists of 3 generation units, 3 loads, 2 tap-changing transformers and 7 lines as shown in Fig. 3. In this study, we assume that this 6-bus system includes two wind farms, each with a generation capacity of 50 MW, located at bus 3 and bus 5 respectively with a 47.8% wind penetration level. More detailed data of this modified system can be found in Appendix, including bus data, load demand data over the 24-hour horizon, line data, tap-changing and phase-shifting transformers data, and generation unit data.

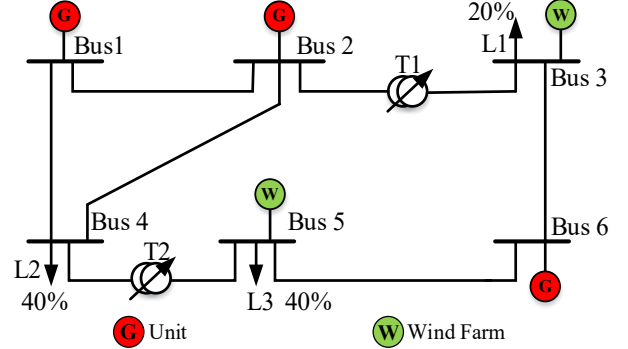


Fig. 3. Topology diagram of the IEEE 6-bus system.

The AC-NCUC model and the proposed solution approach are analysed by implementing four different cases on the modified 6-bus system. These cases are designed to represent different conditions, highlighting the impacts of integrating network constraints and considering uncertain wind power output on UC dispatch decisions in power systems. Each case builds upon the previous one, offering insights into how dispatch decisions evolve from simplified assumptions to fully adaptive robust AC-NCUC decision-making. The four cases are detailed as follows:

- **Case A:** Base UC with the forecasted wind power output, no network constraints considered. This case provides a baseline for comparison. It obtains a simple and traditional UC dispatch decisions, where wind power output is forecasted, and no network constraints are imposed. Case A establishes a reference point to measure the impact of adding network constraints and considering uncertain wind power output. It allows us to observe the operational performance of power systems without the complexity of network constraints and provides insight into the basic operation of the power system.
- **Case B:** This case considers DC network constraints based on Case A with the forecasted wind power output. Case B reflects a more realistic scenario, ensuring the power system security under DC network constraints. In practice, DC network constraints are crucial to the security operation of a power system, as these constraints can influence UC dispatch decisions. By comparing this case with Case A, we can analyze how the inclusion of DC network constraints affects the UC dispatch decisions.
- **Case C:** This case continues to incorporate DC network constraints but also introduces uncertainty in wind power output. Through the comparison with B, we can better understand the impact of wind power output uncertainty on the UC dispatch decisions. As a result, this case enables the system operator to make more reliable and resilient



$[\Delta^t] = 0$  and  $[\Delta^t] = 1$  increases with higher values of  $\Lambda$  and  $\lambda$ . This result shows that a more robust and conservative strategy is determined as the uncertainty increases. To further illustrate this, Fig. 5 shows the specific UC dispatch results under  $\Lambda=0.2$  and  $\lambda=0.5$ . The total cost is \$62,885 when  $[\Delta^t]=0$ , while it rises to \$63,831 when  $[\Delta^t]=1$ . This increase in cost is primarily due to Unit 3 being additionally committed at hour 7 to account for the worst-case scenario.

TABLE III.  
TOTAL COST (\$) OF ADAPTIVE ROBUST UC WITH DC NETWORK CONSTRAINTS AND UNCERTAIN WIND (CASE C) WITH  $[\Delta^t] = 1$

$\Lambda \backslash \lambda$	0.1	0.2	0.3	0.4	0.5
0.1	62,944	63,697	64,460	65,196	65,977
0.2	63,003	63,831	64,637	65,433	66,276
0.3	63,062	63,964	64,808	65,669	67,105
0.4	63,121	64,093	64,990	65,944	67,486
0.5	63,179	64,229	65,167	66,183	67,939
0.6	63,238	64,312	65,344	66,422	68,439
0.7	63,297	64,429	65,521	67,189	68,767
0.8	63,356	64,547	65,696	67,497	69,427
0.9	63,415	64,665	65,911	67,833	69,838
Ref [37]	63,474	64,764	66,090	68,210	70,250

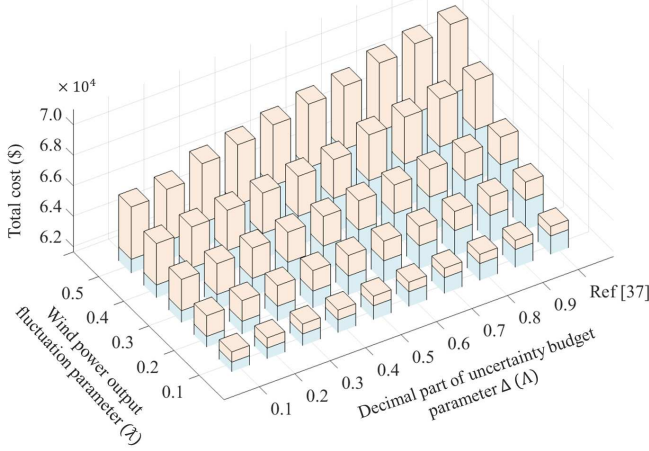


Fig. 4. Comparison of total costs between  $[\Delta^t] = 0$  and  $[\Delta^t] = 1$ .

Hour	1	2	3	4	5	6	7	8	9	10	11	12	13	14	15	16	17	18	19	20	21	22	23	24
Unit	1	2	3	4	5	6	7	8	9	10	11	12	13	14	15	16	17	18	19	20	21	22	23	24
[ $\Lambda$ ]=0, $\Lambda=0.2$ and $\lambda=0.5$ Total Cost: \$62,885																								
1	✓	✓	✓	✓	✓	✓	✓	✓	✓	✓	✓	✓	✓	✓	✓	✓	✓	✓	✓	✓	✓	✓	✓	✓
2	x	x	x	x	x	x	x	x	x	x	x	x	x	x	x	x	x	x	x	x	x	x	x	x
3	x	x	x	x	x	x	✓	✓	✓	✓	✓	✓	✓	✓	✓	✓	✓	✓	✓	✓	✓	✓	✓	✓
[ $\Lambda$ ]=1, $\Lambda=0.2$ and $\lambda=0.5$ Total Cost: \$63,831																								
1	✓	✓	✓	✓	✓	✓	✓	✓	✓	✓	✓	✓	✓	✓	✓	✓	✓	✓	✓	✓	✓	✓	✓	✓
2	x	x	x	x	x	x	x	x	x	x	x	x	x	x	x	x	x	x	x	x	x	x	x	x
3	x	x	x	x	x	x	✓	✓	✓	✓	✓	✓	✓	✓	✓	✓	✓	✓	✓	✓	✓	✓	✓	✓

Fig. 5. Commitment status of units based on different scenarios in Case C.

**Case D:** This case examines the impact of AC network constraints and uncertain wind power on UC dispatch decisions in power systems. Compared to DC network constraints, AC network constraints additionally involve active power constraint (8), reactive power constraint (9), voltage constraint (14), tap-changing transformer constraint (15), and phase-shifting transformer capacities constraint (16). In this case,  $[\Delta^t]$

is set to 1. Table IV and Fig. 6 present the corresponding total costs for varying values of  $\Lambda$  and  $\lambda$ . As expected, the total cost increases as the parameters  $\lambda$  and  $\Lambda$  increase, thus the AC-NCUC dispatch decisions become more robust. This also highlights the flexibility of the proposed model, which allows the system operators to adjust the conservativeness of the dispatch decisions according to their cost budget, enabling a balance between system security and economic costs. In addition, the total costs increase from Case A to Case D, because additional AC constraints are considered to represent a more realistic power system operating environment. For example, comparing Table III to Table IV, it is evident that the total cost in case D is higher than that in case C due to the additional AC constraints.

TABLE IV.  
TOTAL COST (\$) OF AC-NCUC (CASE D) WITH  $[\Delta^t] = 1$

$\Lambda \backslash \lambda$	0.1	0.2	0.3	0.4	0.5
0.1	63,234	63,987	64,835	65,686	66,599
0.2	63,293	64,121	65,037	65,956	66,979
0.3	63,351	64,255	65,239	66,227	67,358
0.4	63,410	64,388	65,441	66,531	67,741
0.5	63,469	64,518	65,643	66,835	68,187
0.6	63,528	64,657	65,845	67,139	68,713
0.7	63,587	64,790	66,047	67,442	69,258
0.8	63,646	64,926	66,249	67,750	69,754
0.9	63,705	65,061	66,463	68,089	70,332
Ref [37]	63,764	65,196	66,691	68,492	70,832

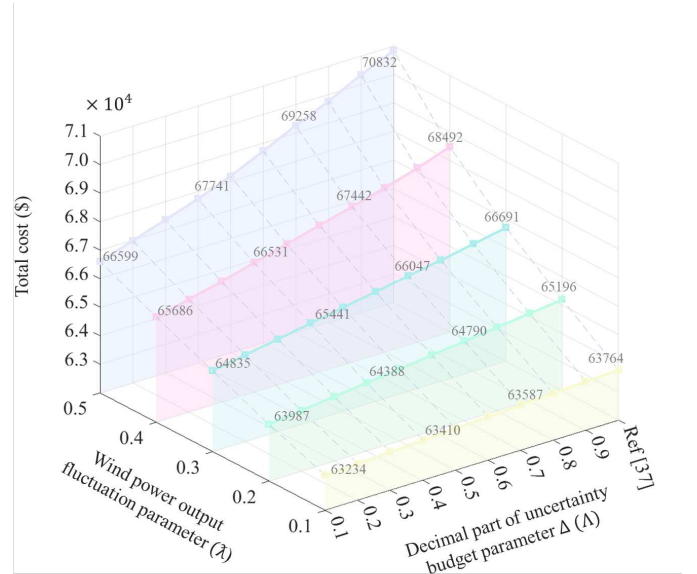


Fig. 6. Total costs under different scenarios based on Case D.

To further analyse AC-NCUC dispatch decisions in different scenarios, Fig.7 shows the commitment status of all units over a 24-hour period. In the scenario with  $\Lambda=0.2$  and  $\lambda=0.5$ , Unit 2 is not committed, and the detailed active power output of three units is shown in Fig.8, where the Wind\* represents the wind power output with considerations of load shedding and wind power curtailment. In contrast, for the scenario with  $\Lambda=0.8$  and  $\lambda=0.5$ , Unit 2 is committed from hours 21 to 24. This indicates that Unit 2 is additionally committed to respond to more

extreme wind power output scenarios. Similarly, when the wind power output deviation  $\lambda$  increases to be 0.6 in the scenario with  $\Lambda=0.8$ , Unit 2 is committed for additional hours 6-20 compared to the scenario with  $\Lambda=0.8$  and  $\lambda=0.5$ . This additional unit commitment is necessary to cover the higher variability of wind power output, leading to an increase in total cost. By dispatching the more expensive Unit 2 during additional hours, the system ensures the security of operations under extreme wind power conditions.

Furthermore, the differences between Case C and Case D reflect the impact of DC and AC network constraints on UC decisions and the total costs. DC network constraints focus solely on active power flows, whereas AC network constraints incorporate additional requirements such as voltage regulation, reactive power management, and transformer operation. These additional constraints significantly influence the UC dispatch decisions in Case D, resulting in higher total costs compared to Case C. For example, Unit 2 is committed more extensively to meet the voltage and reactive power demand, leading to higher unit commitment costs compared to Fig. 5 in Case C. This means that the proposed AC-NCUC model determines more practical dispatch decisions, requiring additional unit commitments to maintain the AC network stability of the power system. The comparison also directly reflects the trade-off between system security and economic costs when making UC dispatch decisions.

Hour	1	2	3	4	5	6	7	8	9	10	11	12	13	14	15	16	17	18	19	20	21	22	23	24
Unit																								
$\Lambda'$  =1, $\Lambda=0.2$ and $\lambda=0.5$ Total Cost: \$66,979																								
1	✓	✓	✓	✓	✓	✓	✓	✓	✓	✓	✓	✓	✓	✓	✓	✓	✓	✓	✓	✓	✓	✓	✓	✓
2	x	x	x	x	x	x	x	x	x	x	x	x	x	x	x	x	x	x	x	x	x	x	x	x
3	✓	✓	✓	✓	✓	✓	✓	✓	✓	✓	✓	✓	✓	✓	✓	✓	✓	✓	✓	✓	✓	✓	✓	✓
$\Lambda'$  =1, $\Lambda=0.8$ and $\lambda=0.5$ Total Cost: \$69,754																								
1	✓	✓	✓	✓	✓	✓	✓	✓	✓	✓	✓	✓	✓	✓	✓	✓	✓	✓	✓	✓	✓	✓	✓	✓
2	x	x	x	x	x	x	x	x	x	x	x	x	x	x	x	x	x	x	x	x	x	x	x	x
3	✓	✓	✓	✓	✓	✓	✓	✓	✓	✓	✓	✓	✓	✓	✓	✓	✓	✓	✓	✓	✓	✓	✓	✓
$\Lambda'$  =1, $\Lambda=0.8$ and $\lambda=0.6$ Total Cost: \$71,972																								
1	✓	✓	✓	✓	✓	✓	✓	✓	✓	✓	✓	✓	✓	✓	✓	✓	✓	✓	✓	✓	✓	✓	✓	✓
2	x	x	x	x	x	x	x	x	x	x	x	x	x	x	x	x	x	x	x	x	x	x	x	x
3	✓	✓	✓	✓	✓	✓	✓	✓	✓	✓	✓	✓	✓	✓	✓	✓	✓	✓	✓	✓	✓	✓	✓	✓

Fig. 7. Commitment status of units based on different scenarios in Case D.

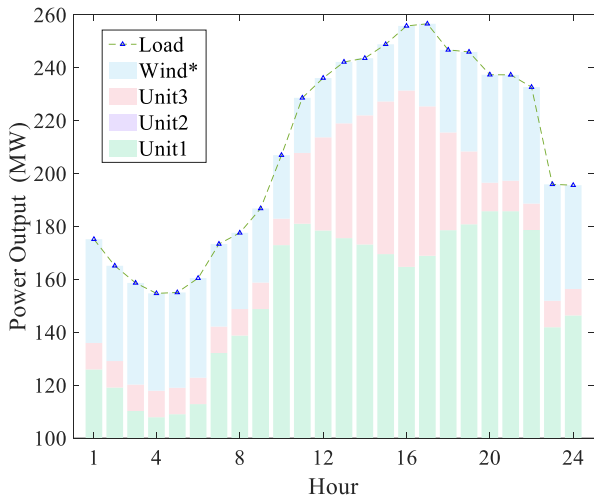


Fig. 8. Active power output of three units in Case D.

## B. IEEE RTS-79 System

In this section, additional case studies are carried out on the modified IEEE-79 system to further demonstrate the effectiveness of our proposed AC-NCUC approach. The topology of this system is shown in Fig. 9. It consists of 24 nodes, 32 generation units, 38 lines, 5 tap-changing transformers, and 17 load buses. In these case studies, we assume the presence of three wind farms at bus 3, 13 and 23 respectively. Each wind farm has a generation capacity of 200 MW, with an overall penetration level of 35%.

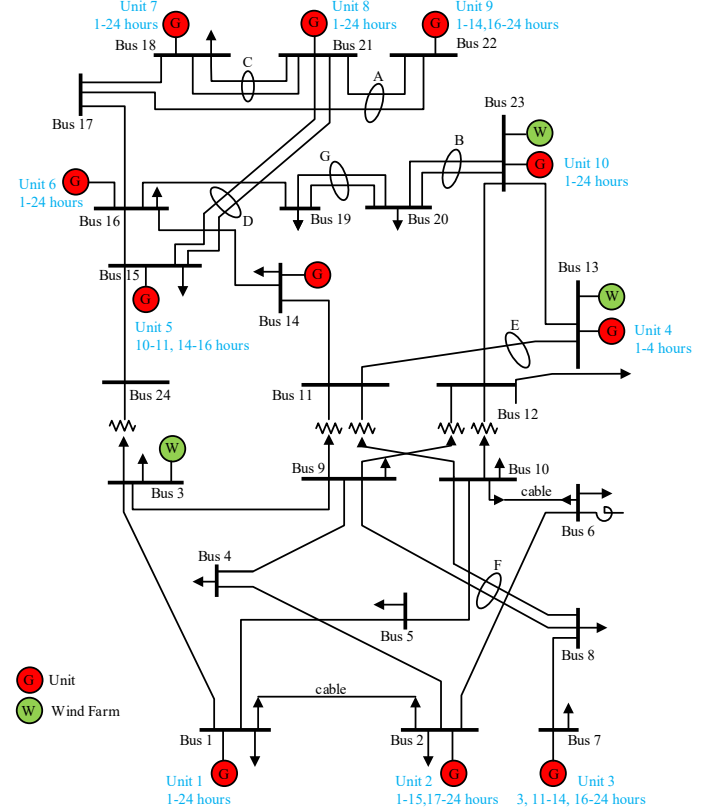


Fig. 9. Topology diagram of the IEEE RTS-79 system.

Tables V-VI present the total costs for various scenarios applied to the IEEE RTS 79 system. It can be seen that the total cost in Case D is relatively higher than that of Case C. For instance, when wind fluctuation and uncertainty budget are  $\lambda=0.1$  and  $\Lambda=0.2$  in Table V, the total cost in Case C is \$452,561, while in Case D it is \$493,582, showing a cost difference of \$41,021. This increase is attributed to the additional AC network constraints enforced by Case D. The incorporation of AC constraints results in more practical dispatch decisions, as it accounts for factors like voltage regulation, reactive power management, and transformer operation to maintain the security and stability of the power system under AC network-constrained conditions. Meanwhile, as expected, the total cost increases as  $\Lambda$  grows, indicating that more extreme wind power output scenarios lead to higher total costs. Similarly, a pattern that emerges is that as  $\lambda$  increases from 0.2 to 0.8 to simulate wind variability with higher power output fluctuation, the costs in both cases show an overall upward trend, although the increase is not always in a strictly linear manner. Fortunately, the system operators can flexibly determine more reasonable UC dispatch decisions based on the uncertainty considerations

of budget cost, which validates the superiority of our proposed AC-NCUC model. In addition, Fig. 9 marks the ON status of all units when  $\lfloor \Delta^t \rfloor = 1$ . Next, we will analyse the commitment status of all units under different uncertainty budget scenarios.

TABLE V.  
TOTAL COST (\$) OF AC-NCUC (CASE D) WITH  $\lfloor \Delta^t \rfloor = 2$  IN RTS-79 SYSTEM

$\Lambda$	$\lambda$	0.1		0.3		0.5	
		Case C	Case D	Case C	Case D	Case C	Case D
0.2	0.2	452,561	493,582	455,335	495,931	457,962	494,244
	0.4	452,566	495,129	455,660	495,841	458,471	498,283
	0.6	452,854	495,703	456,096	496,152	459,178	501,126
	0.8	452,960	495,767	454,475	498,798	459,724	503,322
Ref [37]		452,988	496,081	454,702	501,810	460,130	505,368

TABLE VI.  
TOTAL COSTS (\$) OF AC-NCUC (CASE D) WITH  $\lfloor \Delta^t \rfloor = 1$  IN RTS-79 SYSTEM

$\Lambda$	$\lambda$	0.1		0.3		0.5	
		Case C	Case D	Case C	Case D	Case C	Case D
0.2	0.2	451,798	491,988	453,463	494,074	455,037	493,621
	0.4	451,908	492,311	453,797	494,703	455,605	494,798
	0.6	450,823	494,657	453,946	495,816	456,532	498,851
	0.8	450,974	493,041	454,489	496,622	456,738	500,065
Ref [37]		452,463	495,183	455,113	498,657	457,516	501,024

To analyse the AC-NCUC dispatch decisions, Fig. 10-11 show the commitment status of units for Case C and Case D when wind fluctuation and decimal part of uncertainty budget are  $\lambda = 0.4$ ,  $\Lambda = 0.5$ , but the integer part of uncertainty budget varies between  $\lfloor \Delta^t \rfloor = 1$  and  $\lfloor \Delta^t \rfloor = 2$ , respectively. Fig. 11 takes  $\lfloor \Delta^t \rfloor = 2$  as an example, certain expensive units are committed during specific hours. Specifically, the commitment status of units 1, 2, 3, 5, and 9 differs between Case C and Case D during hours 5 to 24. This is primarily due to the additional AC constraints modelled in Case D, such as reactive power constraints and voltage magnitude constraints, which are not considered in Case C. As a result, some expensive units are committed to mitigate the AC network violations, such as reactive power flow and voltage violations. Comparing Fig. 10 and Fig. 11, the in-service hours and quantities of expensive committed units increase from  $\lfloor \Delta^t \rfloor = 1$  to  $\lfloor \Delta^t \rfloor = 2$ . This reflects the need for additional units to be committed to handle extreme wind scenarios effectively. As  $\lfloor \Delta^t \rfloor$  increases, the system operator dispatches more units and extends these units' operating hours to manage the higher wind power output fluctuation, resulting in the greater impact on system stability and operational costs. In addition, it should be noted that the solution time of the AC-NCUC model increases as the system scale grows, but the solution time remains less than 15 minutes in the IEEE RTS-79 System. This indicates that our solution algorithm has sufficient computational efficiency when handling large-scale system, enabling it to meet the dispatch requirement of the system operator.

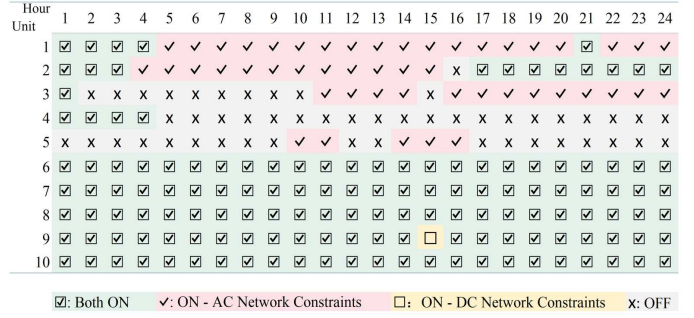


Fig. 10. Commitment status of all units ( $\lfloor \Delta^t \rfloor = 1$ )

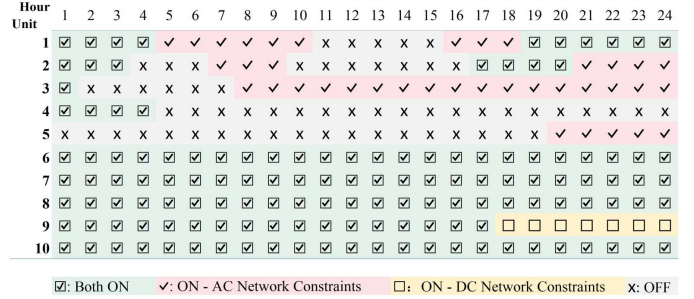


Fig. 11. Commitment status of all units ( $\lfloor \Delta^t \rfloor = 2$ )

## V. CONCLUSION

This paper proposes a novel two-stage adaptive robust AC-NCUC model for power systems with high wind power penetration. The proposed model can be structured as a min-max-min problem, of which the first stage determines UC dispatch decisions, and the second stage minimizes the total operational costs under uncertain wind power output scenarios. By incorporating AC power flow and voltage constraints, the model effectively addresses the interaction between active and reactive power under high levels of wind power fluctuation. A novel feature of this model is its integration of a convex polyhedral uncertainty set to capture the uncertainty of wind power output. This approach accounts for extreme wind power scenarios, ensuring robust UC dispatch decisions. To obtain an optimal dispatch strategy, the Benders' decomposition and Newton-Raphson methods are combined to decompose the origin problem into an outer master problem of DC-UC with inner bilinear decomposition, and hourly AC network security subproblems. This algorithm utilizes Benders cuts derived from the max-min subproblem, as well as the cut of mismatch from AC network violations. Numerical results demonstrate the AC-NCUC model's high effectiveness in making dispatch decisions under extreme wind power output scenarios, as well as its robustness in securing voltage stability by considering AC network constraints under uncertain wind power output conditions.

## APPENDIX

### A. Jacobian Matrix Formulation with Transformer Model

This section provides the control transformer model for the NCUC problem. The control transformer incorporates tap-changing and phase-shifting capabilities, which can accurately represent the electrical behavior of a transformer and to be used in the computation of the Jacobian matrix elements. According to ref. [29], the configuration is illustrated in Fig. A1, and it

connects two buses—tap side  $j$  and non-tap side  $m$ . The complex off-nominal ratio of the phase shifting transformer  $k_T$  captures both tap ratio  $T_{jm}$  and phase angle shift  $\gamma_{jm}$ . More details are given in [29].

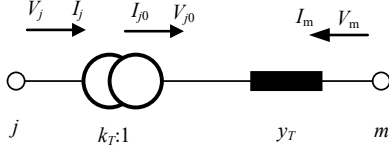


Fig. A1 Configuration of tap-changing and phase-shifting transformers [29].

According to ref. [29], real bus injections  $P_j$  and reactive bus injections  $Q_j$  at bus  $j$  can be formulated as follows:

$$P_j = V_j^2 G_{jj} + V_j \sum_{m \in S_j, j \neq m} V_m \begin{bmatrix} G_{jm} \cos(\delta_j - \delta_m) \\ + B_{jm} \sin(\delta_j - \delta_m) \end{bmatrix} \quad (\text{A1})$$

$$Q_j = -V_j^2 B_{jj} + V_j \sum_{m \in S_j, j \neq m} V_m \begin{bmatrix} G_{jm} \sin(\delta_j - \delta_m) \\ - B_{jm} \cos(\delta_j - \delta_m) \end{bmatrix} \quad (\text{A2})$$

where  $V_j$  and  $\delta_j$  are the voltage magnitude and the voltage angle at bus  $j$ , respectively.  $G_{jm}$  and  $B_{jm}$  are the conductance and the susceptance between buses  $j$  and  $m$ , respectively.  $G_{jj}$  and  $B_{jj}$  are the self-conductance and self-susceptance at bus  $j$ , respectively. In addition,  $S_{jm}$  represents the branches linking buses  $j$  and  $m$ . The partial derivative of (A1) and (A2) with respect to  $\delta$ ,  $V$ ,  $T$ , and  $\gamma$  are defined as follows:

$$\begin{aligned} \mathbf{H} &= \frac{\partial \mathbf{P}}{\partial \delta} & \mathbf{L} &= \frac{\partial \mathbf{P}}{\partial V} & \mathbf{E} &= \frac{\partial \mathbf{P}}{\partial T} & \mathbf{G} &= \frac{\partial \mathbf{P}}{\partial \gamma} \\ \mathbf{M} &= \frac{\partial \mathbf{Q}}{\partial \delta} & \mathbf{J} &= \frac{\partial \mathbf{Q}}{\partial V} & \mathbf{R} &= \frac{\partial \mathbf{Q}}{\partial T} & \mathbf{S} &= \frac{\partial \mathbf{Q}}{\partial \gamma} \end{aligned} \quad (\text{A3})$$

The above Jacobian submatrices ( $\mathbf{H}$ ,  $\mathbf{L}$ ,  $\mathbf{E}$ ,  $\mathbf{G}$ ,  $\mathbf{M}$ ,  $\mathbf{N}$ ,  $\mathbf{R}$  and  $\mathbf{S}$ ) represent the linearized relationship between small variations in the system state and control variables ( $\Delta\delta$ ,  $\Delta V$ ,  $\Delta T$  and  $\Delta\gamma$ ) and corresponding small variations in real and reactive power mismatches.

Then, we can obtain the complex power flow on line  $j - m$ :

$$\begin{aligned} \dot{S}_{L_{jm}} &= V_j^2 (GL_{jj} - jB_{jj}) + V_j V_m (\cos(\delta_j - \delta_m) \\ &+ j \sin(\delta_j - \delta_m)) (GL_{jm} - jBL_{jm}) \end{aligned} \quad (\text{A4})$$

As well as the real and reactive power flow from bus  $j$  to  $m$ :

$$PL_{jm} = V_j^2 GL_{jj} + V_j V_m \begin{bmatrix} GL_{jm} \cos(\delta_j - \delta_m) \\ + BL_{jm} \sin(\delta_j - \delta_m) \end{bmatrix} \quad (\text{A5})$$

$$QL_{jm} = -V_j^2 BL_{jj} + V_j V_m \begin{bmatrix} GL_{jm} \sin(\delta_j - \delta_m) \\ - BL_{jm} \cos(\delta_j - \delta_m) \end{bmatrix} \quad (\text{A6})$$

We can define Jacobian submatrices ( $\mathbf{U}$ ,  $\mathbf{W}$ ,  $\mathbf{Y}$  and  $\mathbf{Z}$ ) to present the linearized relationship between  $\Delta\delta$ ,  $\Delta V$ ,  $\Delta T$  and  $\Delta\gamma$  in relation to small variations in real power flows.

$$\mathbf{U} = \frac{\partial \mathbf{PL}}{\partial \delta} \quad \mathbf{W} = \frac{\partial \mathbf{PL}}{\partial V} \quad \mathbf{Y} = \frac{\partial \mathbf{PL}}{\partial T} \quad \mathbf{Z} = \frac{\partial \mathbf{PL}}{\partial \gamma} \quad (\text{A7})$$

Based on these derivations, we can obtain the Jacobian matrix for the linearized power flow equations.

## B. Data in the modified IEEE 6-bus System

TABLE AI  
BUS DATA

Bus.	$V_{\max}$	$V_{\min}$	Initial-vol	Initial angle
1	1.10	0.95	1.00	0
2	1.15	0.90	1.00	0
3	1.15	0.90	1.00	0
4	1.15	0.90	1.00	0
5	1.15	0.90	1.00	0
6	1.15	0.90	1.00	0

TABLE AII  
TRANSMISSION LINE DATA

Line	From	To	Resistance	Reactance	$F_{\max}$
1	1	2	0.0050	0.170	150
2	1	4	0.0030	0.258	75
3	2	3	0.0000	0.037	100
4	2	4	0.0070	0.197	100
5	3	6	0.0005	0.018	90
6	4	5	0.0000	0.037	90
7	5	6	0.0020	0.140	90

TABLE AIII  
TAP-CHANGING AND PHASE-SHIFTING TRANSFORMERS DATA

Tap	From	To	Reactance	$T_{\min}$	$T_{\max}$	$\gamma_{\max}$	$\gamma_{\min}$
T1	2	3	0.037	0.90	1.10	60°	-30°
T2	4	5	0.037	0.90	1.10	60°	-30°

TABLE AIV  
GENERATION UNIT DATA

U	Bus	Unit Cost Coefficients			$\bar{P}$	$\underline{P}$	$\bar{Q}$	$\underline{Q}$	$T^{off}$	$T^{on}$	DR/UR	SU/SD
		Constant term	Linear term	Quadratic term								
1	1	176.9	13.5	0.0004	220	100	1000	-100	4	4	55	180
2	2	129.9	32.6	0.0001	100	10	1000	-100	2	3	50	360
3	6	137.4	17.6	0.005	100	10	1000	-100	1	1	20	60

## REFERENCES

- [1] IRENA, "Record Growth in Renewables, but Progress Needs to be Equitable," 2024.
- [2] "IRENA. Renewable Capacity Statistics 2018[R]," 2019.
- [3] M. Wiatros-Motyka, N. Fulghum, and D. Jones, "Global Electricity Review 2024," 2024.
- [4] S. Zhang, G. Pan, B. Li, W. Gu, J. Fu, and Y. Sun, "Multi-Timescale Security Evaluation and Regulation of Integrated Electricity and Heating System," *IEEE Transactions on Smart Grid*, pp. 1-1, 2024.
- [5] L. Che, X. Liu, and Z. Li, "An Intra-Interval Security Risk Regarding Regulation Burden Due to Wind Variation in High-Wind-Penetrated Power Systems," *IEEE Transactions on Power Systems*, vol. 33, no. 3, pp. 3213-3216, 2018.
- [6] J. Yan, H. Zhang, Y. Liu, S. Han, and L. Li, "Uncertainty estimation for wind energy conversion by probabilistic wind turbine power curve modelling," *Applied Energy*, vol. 239, pp. 1356-1370, 2019/04/01/ 2019.
- [7] H. Pandžić, Y. Dvorkin, T. Qiu, Y. Wang, and D. S. Kirschen, "Toward Cost-Efficient and Reliable Unit Commitment Under Uncertainty," *IEEE Transactions on Power Systems*, vol. 31, no. 2, pp. 970-982, 2016.
- [8] Y. Zhang and G. B. Giannakis, "Distributed Stochastic Market Clearing With High-Penetration Wind Power," *IEEE Transactions on Power Systems*, vol. 31, 04/13 2015.
- [9] C. Wang and Y. Fu, "Fully Parallel Stochastic Security-Constrained Unit Commitment," *IEEE Transactions on Power Systems*, vol. 31, pp. 1-11, 11/10 2015.
- [10] L. Wu, M. Shahidehpour, and Z. Li, "Comparison of Scenario-Based and Interval Optimization Approaches to Stochastic SCUC," *IEEE Transactions on Power Systems - IEEE TRANS POWER SYST*, vol. 27, pp. 913-921, 05/01 2012.
- [11] E. Du, N. Zhang, C. Kang, and Q. Xia, "Scenario Map-Based Stochastic Unit Commitment," *IEEE Transactions on Power Systems*, vol. PP, pp. 1-1, 01/30 2018.
- [12] A. Papavasiliou, S. S. Oren, and R. P. O. Neill, "Reserve Requirements for Wind Power Integration: A Scenario-Based Stochastic Programming Framework," *IEEE Transactions on Power Systems*, vol. 26, no. 4, pp. 2197-2206, 2011.
- [13] C. Wang, F. Liu, J. Wang, F. Qiu, W. Wei, and S. Mei, "Robust Risk-Constrained Unit Commitment with Large-scale Wind Generation: An Adjustable Uncertainty Set Approach," *Mathematics*, 2015.
- [14] B. Hu and L. Wu, "Robust SCUC Considering Continuous/Discrete Uncertainties and Quick-Start Units: A Two-Stage Robust Optimization With Mixed-Integer Recourse," *IEEE Transactions on Power Systems*, vol. 31, pp. 1-13, 04/30 2015.
- [15] H. Ye and Z. Li, "Robust Security-Constrained Unit Commitment and Dispatch With Recourse Cost Requirement," *IEEE Transactions on Power Systems*, vol. 31, no. 5, pp. 3527-3536, 2016.
- [16] Y. An and B. Zeng, "Exploring the Modeling Capacity of Two-Stage Robust Optimization: Variants of Robust Unit Commitment Model," *Power Systems, IEEE Transactions on*, vol. 30, pp. 109-122, 07/01 2015.
- [17] H. Ye and Z. Li, "Robust security-constrained unit commitment and dispatch with recourse cost requirement," *IEEE Transactions on Power Systems*, vol. 31, no. 5, pp. 3527-3536, 2015.
- [18] H. Dashti, A. Conejo, R. Jiang, and J. Wang, "Weekly Two-Stage Robust Generation Scheduling for Hydrothermal Power Systems," *IEEE Transactions on Power Systems*, pp. 1-11, 01/08 2016.
- [19] I. Blanco and J. M. Morales, "An Efficient Robust Solution to the Two-Stage Stochastic Unit Commitment Problem," *IEEE Transactions on Power Systems*, vol. 32, no. 6, pp. 4477-4488, 2017.
- [20] J. M. Morales, S. Pineda, A. J. Conejo, and M. Carrion, "Scenario Reduction for Futures Market Trading in Electricity Markets," *IEEE Transactions on Power Systems*, vol. 24, no. 2, pp. 878-888, 2009.
- [21] X. Zhu, Z. Yu, and X. Liu, "Security Constrained Unit Commitment with Extreme Wind Scenarios," *Journal of Modern Power Systems and Clean Energy*, vol. 8, no. 3, pp. 464-472, 2020.
- [22] R. A. Jabr, "Robust Transmission Network Expansion Planning With Uncertain Renewable Generation and Loads," *IEEE Transactions on Power Systems*, vol. 28, no. 4, pp. 4558-4567, 2013.
- [23] C. Peng, P. Xie, L. Pan, and R. Yu, "Flexible Robust Optimization Dispatch for Hybrid Wind/Photovoltaic/Hydro/Thermal Power System," *IEEE Transactions on Smart Grid*, vol. 7, no. 2, pp. 751-762, 2016.
- [24] D. Bertsimas, E. Litvinov, X. Sun, J. Zhao, and T. Zheng, "Adaptive Robust Optimization for the Security Constrained Unit Commitment Problem," *IEEE Transactions on Power Systems*, vol. 28, pp. 52-63, 02/01 2013.
- [25] F. Verástegui, L. Á. D. E. Olivares, M. Negrete-Pincetic, and P. Gazmuri, "An Adaptive Robust Optimization Model for Power Systems Planning With Operational Uncertainty," *IEEE Transactions on Power Systems*, vol. 34, no. 6, pp. 4606-4616, 2019.
- [26] Z. Li, W. Wu, M. Shahidehpour, and B. Zhang, "Adaptive Robust Tie-Line Scheduling Considering Wind Power Uncertainty for Interconnected Power Systems," *IEEE Transactions on Power Systems*, vol. 31, no. 4, pp. 2701-2713, 2016.
- [27] Q. P. Zheng, J. Wang, and A. L. Liu, "Stochastic Optimization for Unit Commitment—A Review," *IEEE Transactions on Power Systems*, vol. 30, no. 4, pp. 1913-1924, 2015.
- [28] P. Pourbeik, P. S. Kundur, and C. W. Taylor, "The anatomy of a power grid blackout - Root causes and dynamics of recent major blackouts," *IEEE Power and Energy Magazine*, vol. 4, no. 5, pp. 22-29, 2006.
- [29] F. Yong, M. Shahidehpour, and L. Zuyi, "Security-constrained unit commitment with AC constraints," *IEEE Transactions on Power Systems*, vol. 20, no. 3, pp. 1538-1550, 2005.
- [30] A. Nasri, S. J. Kazempour, A. J. Conejo, and M. Ghandhari, "Network-Constrained AC Unit Commitment

Under Uncertainty: A Benders' Decomposition Approach," *IEEE Transactions on Power Systems*, vol. 31, no. 1, pp. 412-422, 2016.

- [31] N. Amjady, S. Dehghan, A. Attarha, and A. J. Conejo, "Adaptive Robust Network-Constrained AC Unit Commitment," *IEEE Transactions on Power Systems*, vol. 32, no. 1, pp. 672-683, 2017.
- [32] X. Zhang, T. Ding, H. Zhang, Z. Zeng, P. Siano, and M. Shahidehpour, "A Two-Stage Stochastic Unit Commitment With Mixed-Integer Recourses for Nuclear Power Plants to Accommodate Renewable Energy," *IEEE Transactions on Sustainable Energy*, vol. 15, no. 2, pp. 859-870, 2024.
- [33] D. Bertsimas, E. Litvinov, X. A. Sun, J. Zhao, and T. Zheng, "Adaptive Robust Optimization for the Security Constrained Unit Commitment Problem," *IEEE Transactions on Power Systems*, vol. 28, no. 1, pp. 52-63, 2013.
- [34] A. Gholami, T. Shekari, and S. Grijalva, "Proactive Management of Microgrids for Resiliency Enhancement: An Adaptive Robust Approach," *IEEE Transactions on Sustainable Energy*, vol. 10, no. 1, pp. 470-480, 2019.
- [35] T. N. Santos and A. L. Diniz, "Feasibility and optimality cuts for the MultiStage benders decomposition approach: Application to the network constrained hydrothermal scheduling," in *2009 IEEE Power & Energy Society General Meeting*, 2009, pp. 1-8.
- [36] A. Sun and A. Lorca, "Adaptive robust optimization for daily power system operation," in *2014 Power Systems Computation Conference*, 2014, pp. 1-9.
- [37] R. Jiang, J. Wang, and Y. Guan, "Robust Unit Commitment With Wind Power and Pumped Storage Hydro," *IEEE Transactions on Power Systems*, vol. 27, no. 2, pp. 800-810, 2012.



**Siqi Wang** received the B.Sc. degree in aircraft design and engineering from Nanjing University of Aeronautics and Astronautics, Nanjing, China, in 2014, and received the M.Sc. and Ph.D. degrees in autonomous vehicle dynamics and control from Cranfield University, U.K., in 2015 and 2020. She is currently an Associate Professor with Institute of Electrical Engineering, Chinese Academy of Sciences, Beijing, China. From 2020 to 2023, she was a Research Fellow with Cranfield University, U.K. From 2023 to 2024, she was a lecturer with the School of Physics, Engineering and Computer Science, University of Hertfordshire, U.K. Her research interests include energy management strategies for hybrid renewable power systems, AI for transport and energy systems.



**Xin Zhang** (Senior Member, IEEE) received the B.Eng. degree in automation and control systems from Shandong University, Jinan, China, in 2007, and the M.Sc. and Ph.D. degrees in electrical power engineering from The University of Manchester, Manchester, U.K., in 2007 and 2010, respectively.

Currently, he is a Professor of Control and Power Systems with the School of Electrical and Electronic Engineering, University of Sheffield, Sheffield, U.K. From 2011 to 2019, he was with National Grid Electricity System Operator, Wokingham, U.K. From 2019 to 2021, he was a Senior Lecturer with Cranfield University, U.K. From 2021 to 2023, he was an Associate Professor with Brunel University London, U.K. His research interests include power system control and operation, cyber-physical power systems modelling and digital simulation, and grid-integrated transport electrification. In 2022, he was a recipient of U.K. Engineering and Physical Sciences Research Council (EPSRC) New Investigator Award and U.K. Research and Innovation (UKRI) Future Leaders Fellowship.



**Min Du** (Member, IEEE) received the B.Sc. degree from the School of Electrical and Information Engineering, Wuhan Institute of Technology, Wuhan, China, in 2016, and the M.Sc. and Ph.D. degrees from the College of Electrical and Information Engineering, Hunan University, Changsha, China, in 2019 and 2023, respectively. He is currently a

Postdoctoral Research Associate with The University of Sheffield, U.K. His research interests include cyber-physical power systems, cybersecurity, and resilience.



**Wei Pei** (Member, IEEE) received the B.S. and M.S. degrees in Electrical Engineering from Tianjin University, Tianjin, China, in 2002 and 2005, respectively, and the Ph.D. degree in Electrical Engineering from the Institute of Electrical Engineering, Chinese Academy of Sciences in 2008. He is currently a Professor and the Director of the Power grid technology laboratory, Institute of Electrical Engineering, Chinese Academy of Sciences. His research interests include AC/DC microgrids, stability and control of power systems with high level power electronics.